Available online at www.sciencedirect.com
ScienceDirect
International Journal of Heat and Fluid Flow 27 (2006) 838–851
International Journal of HEAT AND FLUID FLOW
www.elsevier.com/locate/ijhff

Nonlinear eddy diffusivity model for wall-bounded flow with arbitrary rotating axes

H. Hattori [a,*], N. Ohiwa [b], Y. Nagano [a]

[a] Department of Mechanical Engineering, Nagoya Institute of Technology, Gokiso-cho, Showa-ku, Nagoya 466-8555, Japan
[b] Department of Engineering Physics, Electronics and Mechanics, Nagoya Institute of Technology, Nagoya, Japan

Received 2 October 2005; received in revised form 29 January 2006; accepted 4 March 2006
Available online 15 June 2006

Abstract

Rotating flows have been encountered in many engineering-relevant applications such as a flow in turbomachinery. Recently, rotating channel flows with arbitrary rotating axes have been investigated by direct numerical simulation (DNS). Although numerical studies of spanwise rotating channel flow have been reported, there are few reports on streamwise and wall-normal rotating channel flows. In the present study, first, we conducted DNS of various rotational channel flows in order to understand phenomena of rotating wall-bounded flows and to make databases for turbulence modelling. It is found from the DNS results that cases of streamwise rotating channel flow which have a mean spanwise velocity caused by rotation involve the counter gradient turbulent diffusion. Thus, since it is well-known that the conventional eddy diffusivity turbulence model (EDM) cannot predict this case, we have to consider the reconstruction of a nonlinear eddy viscosity turbulence model (NLEDM) based on a cubic model. Consequently, we evaluated existing nonlinear eddy viscosity turbulence models based on our DNS of streamwise and wall-normal rotating channel flows. Using the results of evaluation, we have improved the modeled expression for Reynolds stress, in which a new cubic-type nonlinear eddy viscosity model has been proposed. The proposed nonlinear two-equation turbulence model can accurately predict rotating channel flows with arbitrary rotating axes.

Keywords: Nonlinear eddy diffusivity model; Turbulence modelling; Turbulence; Rotational flow; Arbitrary rotating axes; Direct numerical simulation

1. Introduction

Rotating flows have been encountered in many engineering-relevant applications such as a flow in turbomachinery. Recently, a turbulence model has been improved for analysis of a turbulent flow with rotation. In particular, in order to conduct more precise analysis of a rotating turbulent flow, a nonlinear two-equation model is required (Nagano and Hattori, 2002), in which rotating channel flows with spanwise rotations are predicted accurately. On the other hand, rotating channel flows with arbitrary rotating axes have been investigated by direct numerical simulation (DNS). Although DNS studies on spanwise rotating channel flow have been reported (Nagano and Hattori, 2002; Kristoffersen and Andersson, 1993; Lamballais et al., 1996), there are few reports dealing with streamwise and wall-normal rotating channel flows (e.g., Oberlack et al., 1999; Wu and Kasagi, 2004).

In the present study, in order to obtain fundamental statistics on rotating channel flows with arbitrary rotating axes, DNS has been conducted using the spectral method. At the same time, we have made a DNS database for the evaluation of turbulence models. DNSs provide detailed turbulence quantities which are difficult to obtain from measurements, and also provide the budget of the turbulent transport equations. In particular, turbulent diffusion and dissipation terms in the turbulent transport equation can be obtained from DNSs, which are essential to construct a turbulence model. Based on the present DNS of streamwise and wall-normal rotating channel flows, existing nonlinear two-equation turbulence models have been

* Corresponding author. Tel./fax: +81 52 735 5359.
E-mail address: hattori@nitech.ac.jp (H. Hattori).

0142-727X/$ - see front matter © 2006 Elsevier Inc. All rights reserved.
doi:10.1016/j.ijheatfluidflow.2006.03.010

Nomenclature

b_{ij}	anisotropy tensor, $=\overline{u_iu_j}/2k-\delta_{ij}/3$
k	turbulence energy, $=\overline{u_iu_i}/2$
n	local coordinate normal to wall surface
n^*	nondimensional distance between point and nearest point on whole surface, $=u_\varepsilon n/\nu$
$\overline{P}$, p	mean and fluctuating static pressure
Re_b	Reynolds number based on bulk velocity, $=2\overline{U}_b\delta/\nu$
Re_τ	Reynolds number based on friction velocity, $=u_\tau\delta/\nu$
Ro	Rotation number based on bulk velocity and angular velocity, $=2\Omega\delta/\overline{U}_m$
Ro_τ	Rotation number based on friction velocity, $=2\Omega\delta/u_\tau$
R_t	turbulent Reynolds number, $=k^2/\nu\varepsilon$
S_{ij}	strain-tensor, $=(\partial\overline{U}_i/\partial x_j+\partial\overline{U}_j/\partial x_i)/2$
t	time
$\overline{U}$, $\overline{V}$, $\overline{W}$	mean velocity in x-, y- and z-directions, respectively
u, v, w	turbulent fluctuation in x-, y- and z-directions, respectively
$\overline{U}_b$	bulk velocity
$\overline{U}_i$	mean velocity in x_i-direction
u_i	turbulent fluctuation in x_i-direction
u_τ	friction velocity, $=\sqrt{\tau_w/\rho}$
u_ε	Kolmogorov velocity scale, $=(\nu\varepsilon)^{1/4}$
x_i	Cartesian coordinate in i-direction
x, y, z	Cartesian coordinate in streamwise, wall-normal and spanwise directions, respectively
y^+	nondimensional distance from wall surface, $=u_\tau y/\nu$
W_{ij}	absolute vorticity tensor, $=\Omega_{ij}-\epsilon_{ijm}\Omega_m=(\partial\overline{U}_i/\partial x_j-\partial\overline{U}_j/\partial x_i)/2-\epsilon_{ijm}\Omega_m$

Greek symbols

δ	half-width of channel
δ_{ij}	Kronecker delta
ε	dissipation rate of turbulence energy, $=\nu\overline{(\partial u_i/\partial x_j)(\partial u_i/\partial x_j)}$
ϵ_{ijk}	Eddington's epsilon
ν, ν_t	kinematic and eddy viscosities
ρ	density
Ω_{ij}	vorticity tensor, $=(\partial\overline{U}_i/\partial x_j-\partial\overline{U}_j/\partial x_i)/2$
τ_w	wall shear stress
$\overline{(\,)}$	ensemble- or time-averaged value
$(\,)^+$	normalization by inner variables (u_τ, t_τ, ν)
D/Dt	substantial derivative, $=\partial/\partial t+\overline{U}_j\partial/\partial x_j$

evaluated. Using the results of evaluation, we improve the modeled expression for Reynolds stress by proposing a new nonlinear two-equation model for rotating channel flows with arbitrary rotating axes.

2. Governing equations in rotational coordinate system

We consider a fully-developed turbulent channel flow with rotation at a constant angular velocity as shown in Fig. 1. The governing equations for an incompressible rotating channel flow in reference frame rotational coordinates can be described in the following dimensionless forms:

$$\frac{\partial u_i^+}{\partial x_i^+}=0 \tag{1}$$

$$\frac{Du_i^+}{Dt^+}=-\frac{\partial p_{eff}^+}{\partial x_i^+}+\frac{1}{Re_\tau}\frac{\partial^2 u_i^+}{\partial x_j^+\partial x_j^+}-\epsilon_{ik\ell}Ro_{\tau k}u_\ell^+ \tag{2}$$

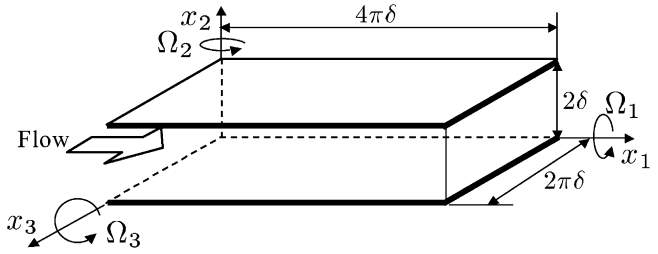

Fig. 1. Rotating channel flow and coordinate system.

where the rotation number $Ro_{\tau k}$ is defined as $2\Omega_k\delta/u_\tau$. The centrifugal force can be included in the effective pressure $p_{eff}^+(=p_s^+-Ro^2r_c^2/8)$, if fluid properties are constant, where p_s^+ is the normalized static pressure, $Ro=(Ro_jRo_j)^{1/2}$ is the absolute rotation number, and r_c is the dimensionless distance from the rotating axis (Wu and Kasagi, 2004). The spectral method is used for the DNS (see Nagano and Hattori, 2003). The computational conditions are listed in Table 1. The boundary conditions are nonslip conditions for the walls as well as periodic conditions in the streamwise and spanwise directions.

The Reynolds-averaged equations for the turbulence model can be written as follows:

$$\frac{\partial\overline{U}_i}{\partial x_i}=0 \tag{3}$$

$$\frac{D\overline{U}_i}{Dt}=-\frac{1}{\rho}\frac{\partial\overline{P}_{eff}}{\partial x_i}+\frac{\partial}{\partial x_j}\left(\nu\frac{\partial\overline{U}_i}{\partial x_j}-\overline{u_iu_j}\right)-2\epsilon_{ik\ell}\Omega_k\overline{U}_\ell \tag{4}$$

Table 1
Methods for direct numerical simulation

Grid		Regular grid
Time advancement	Viscosity term	Crank–Nicolson method
	Other terms	Adams–Bashforth method
Spatial scheme		Spectral method
Grid points ($x_1\times x_2\times x_3$)		$64\times65\times64$
Computational volume		$4\pi\delta\times2\delta\times2\pi\delta$

$$\overline{u_i u_j} = \frac{2}{3}k\delta_{ij} - 2C_0 \nu_t S_{ij} + \text{High order terms} \tag{5}$$

$$\nu_t = C_\mu f_\mu \frac{k^2}{\varepsilon} \tag{6}$$

where the quadratic modeled expression for Reynolds stress applying the rotational turbulent flow in Eq. (5) was proposed by Nagano and Hattori (2002) as follows:

$$\overline{u_i u_j} = \frac{2}{3}k\delta_{ij} - \frac{1}{f_R}2\nu_t S_{ij} + \frac{4C_D}{f_R}k\tau_{Ro}^2 \times \left[(S_{ik}W_{kj} - W_{ik}S_{kj}) - \left(S_{ik}S_{kj} - \frac{\delta_{ij}}{3}S_{mn}S_{mn}\right)\right] + Q_w \tag{7}$$

where $\tau_{Ro} = \nu_t/k$ is the characteristic time-scale, C_D is the model constant, and f_R is the model function. The last term of the right-hand side is introduced to reproduce the wall-limiting behaviour and the anisotropy of Reynolds normal stress components (Hattori and Nagano, 2004) given as follows:

$$Q_w = \frac{4C_D}{f_R}k\tau_{R_w}^2\left[(S_{ik}W_{kj} - W_{ik}S_{kj}) - \left(S_{ik}S_{kj} - \frac{\delta_{ij}}{3}S_{mn}S_{mn}\right)\right] \tag{8}$$

where τ_{R_w} is the characteristic time-scale for reproducing the wall-limiting behaviour and the anisotropy of Reynolds normal stress components.

The transport equations of turbulence quantities, i.e., turbulence energy, k, and dissipation rate of k, ε, which compose the eddy diffusivities, can be given as follows:

$$\frac{Dk}{Dt} = \nu\frac{\partial^2 k}{\partial x_j \partial x_j} + T_k + \Pi_k + P_k - \varepsilon \tag{9}$$

$$\frac{D\varepsilon}{Dt} = \nu\frac{\partial^2 \varepsilon}{\partial x_j \partial x_j} + T_\varepsilon + \Pi_\varepsilon + \frac{\varepsilon}{k}(C_{\varepsilon 1}P_k - C_{\varepsilon 2}f_\varepsilon \varepsilon) + E + R \tag{10}$$

where T_k and T_ε are turbulent diffusion terms, Π_k and Π_ε are pressure diffusion terms, and P_k $(= -\overline{u_i u_j}\overline{U}_{i,j})$ is production term. E is an extra term, and R is a rotation-influenced additional term (Nagano and Hattori, 2002).

3. Discussion of DNS results in view of turbulence modelling

In order to determine improvements in the expression of rotating, wall-bounded turbulent shear flows, DNSs of fully developed channel flows with streamwise, wall-normal and spanwise rotation are carried out using the spectral method (Nagano and Hattori, 2003) for the 15 cases indicated in Table 2. DNS results of cases for STR1–STR5 and WNR1–WNR5 are shown in Figs. 2 and 3, respectively (Case 3 is not shown here). In these cases, the spanwise mean velocity appears to be caused by a rotational effect, which increases with the increase in rotation number in both cases. In particular, with increase in the spanwise mean velocity of Case 2, a streamwise mean velocity decreases due to the exchange momentum between the streamwise and spanwise velocity as in the following equations obtained by Eq. (4):

Table 2
Computational conditions

Re_τ	150				
Case 1: Streamwise rotation					
	STR1	STR2	STR3	STR4	STR5
$Ro_{\tau 1}$	1.0	2.5	7.5	10.0	15.0
Case 2: Wall-normal rotation					
	WNR1	WNR2	WNR3	WNR4	WNR5
$Ro_{\tau 2}$	0.01	0.02	0.05	0.1	0.3
Case 3: Spanwise rotation					
	SPR1	SPR2	SPR3	SPR4	SPR5
$Ro_{\tau 3}$	0.0	0.75	1.5	3.0	5.0

$$0 = -\frac{1}{\rho}\frac{\partial \overline{P}}{\partial x} + \frac{\partial}{\partial y}\left(\nu\frac{\partial \overline{U}}{\partial y} - \overline{uv}\right) - 2\Omega\overline{W} \tag{11}$$

$$0 = \frac{\partial}{\partial y}\left(\nu\frac{\partial \overline{W}}{\partial y} - \overline{vw}\right) + 2\Omega\overline{U} \tag{12}$$

Therefore, in order to predict the flow of Case 2 exactly, the spanwise mean velocity should be reproduced by a turbulence model. Note that the wall-normal rotating DNS (Case 2) of Wu and Kasagi (2004) was carried out on constant streamwise mean velocity condition, but the present DNS does not maintain the constant velocity. Thus, the Reynolds shear stress, $\overline{uv}$, tends to decrease remarkably with the increase in rotational number as shown in Fig. 3(b).

On the other hand, it is found from DNS results that cases of streamwise rotating channel flow (Case 1) involve the counter gradient turbulent diffusion in the spanwise direction shown in Fig. 2. In view of turbulence modelling, this fact clearly demonstrates that the linear EDM and the quadratic NLEDM cannot be applied to calculate the case of a streamwise rotating channel flow. Thus, the following modeled Eq. (13) employed in the linear EDM and the quadratic NLEDM can not clearly express a counter gradient turbulent diffusion

$$-\overline{vw} = \nu_t\frac{\partial \overline{W}}{\partial y} \tag{13}$$

where the Reynolds shear stresses of a quadratic NLEDM are expressed identical to a linear model. Also, it is noted that the rotational term does not appear in the momentum equation of a fully-developed streamwise rotating channel flow indicated as Eq. (16), in which the rotational effect is included implicitly in the Reynolds shear stress in the same manner as the spanwise rotational flow (Nagano and Hattori, 2002). Therefore, a cubic NLEDM or Reynolds stress equation model (RSM) should be used for the calculation of streamwise rotating channel flows as follows:

$$0 = -\frac{1}{\rho}\frac{\partial \overline{P}}{\partial x} + \frac{\partial}{\partial y}\left(\nu\frac{\partial \overline{U}}{\partial y} - \overline{uv}\right) \tag{14}$$

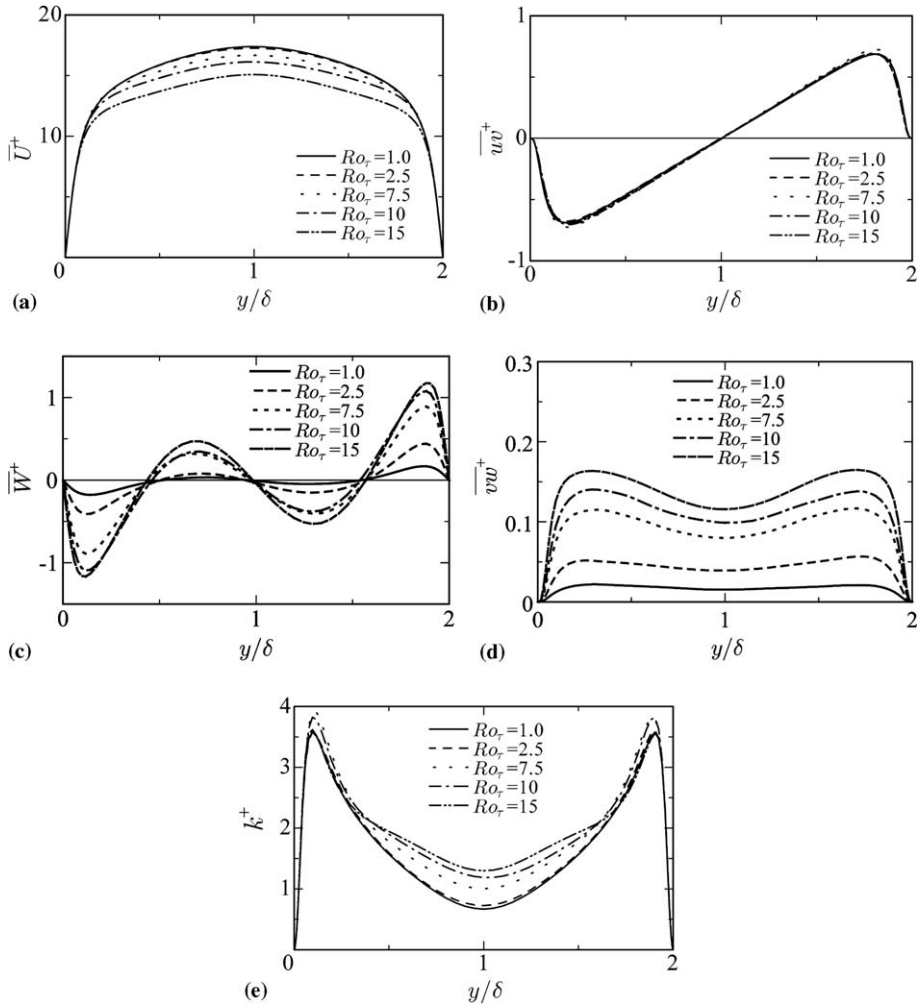

Fig. 2. DNS results of streamwise rotating flows (Case 1): (a) streamwise mean velocities, (b) Reynolds shear stresses, $\overline{uv}$, (c) spanwise mean velocities, (d) Reynolds shear stresses, $\overline{vw}$ and (e) turbulence energy.

$$0 = -\frac{1}{\rho}\frac{\partial \overline{P}}{\partial y} - \frac{\partial \overline{v^2}}{\partial y} + 2\Omega \overline{W} \tag{15}$$

$$0 = \frac{\partial}{\partial y}\left(\nu \frac{\partial \overline{W}}{\partial y} - \overline{vw}\right) \tag{16}$$

3.1. Evaluations of existing turbulence models in rotating wall-bounded flows

Fig. 4 shows the assessment result using the present DNS of two-equation models with NLEDM in the case of streamwise rotating channel flow. The evaluated models are a cubic model by Craft et al. (1996) (hereinafter referred to as NLCLS) and a quadratic model by Nagano and Hattori (2002) (NLHN). Obviously, the quadratic model cannot reproduce this flow as mentioned in the previous section. The cubic model indicates overprediction of mean streamwise velocity, $\overline{U}$, and underpredicts the Reynolds shear stress, $\overline{vw}$, in the case of a higher rotating number. The wall-limiting behaviour of Reynolds stress components is shown in Fig. 4(f). Although the NLHN model is modelled to satisfy the wall-limiting behaviour of the Reynolds stress component in the wall-normal direction in spanwise rotational flow, it can be seen that the model does not reproduce the wall-limiting behaviour.

Evaluations of wall-normal rotating flows predicted by the NLCLS and the NLHN models are indicated in Fig. 5. In this case, it can be seen that the NLHN accurately reproduces turbulent quantities. Thus, one may consider that streamwise rotating flows can be predicted using a quadratic nonlinear model. However, the wall-limiting behaviour of the Reynolds stress component in the wall-normal direction is not predicted in the vicinity of the wall shown in Fig. 5(f).

3.2. Reconstruction of NLEDM

From these results, we propose a cubic NLEDM in a two-equation turbulence model which can adequately predict rotational channel flows with arbitrary rotating axes, in which a modelling of wall-limiting behaviour of Reynolds stress components is also considered.

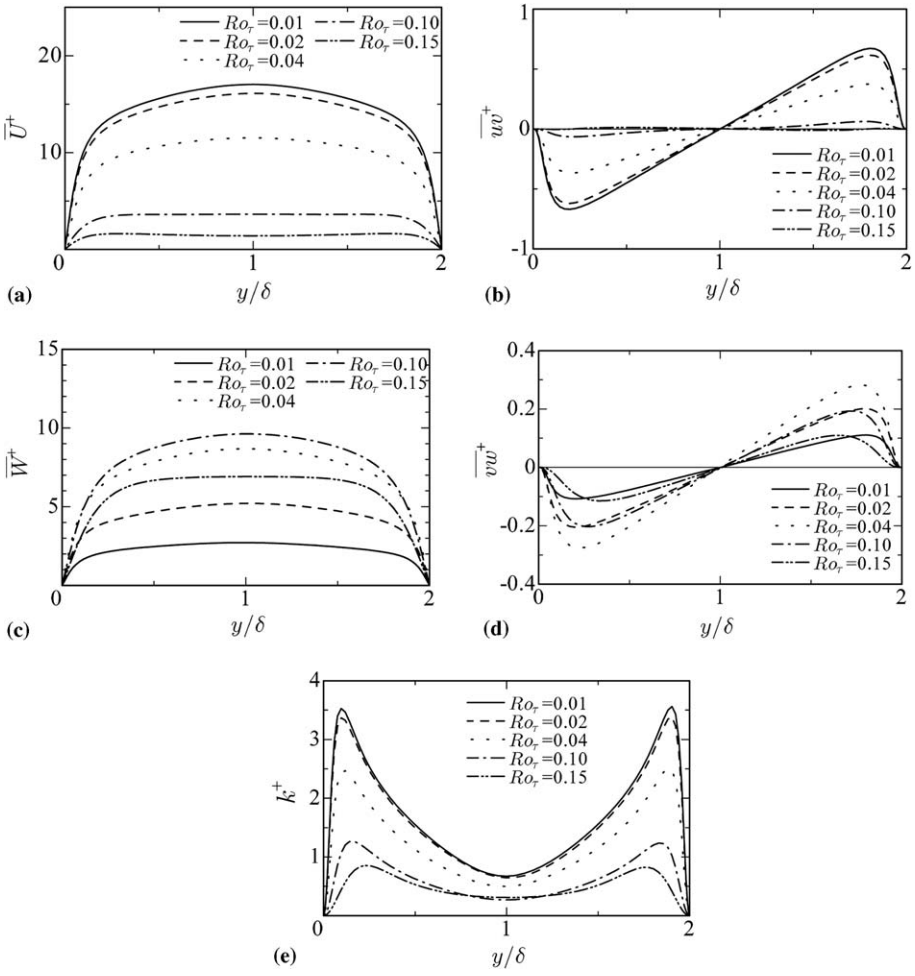

Fig. 3. DNS results of wall-normal rotating flows (Case 2): (a) streamwise mean velocities, (b) Reynolds shear stresses, $\overline{uv}$, (c) spanwise mean velocities, (d) Reynolds shear stresses, $\overline{vw}$ and (e) turbulence energy.

The transport equation of Reynolds stress with the Coriolis term is given as follows:

$$\frac{D\overline{u_i u_j}}{Dt} = D_{ij} + T_{ij} + P_{ij} + C_{ij} + \Phi_{ij} - \varepsilon_{ij} \tag{17}$$

where D_{ij} is a molecular diffusion term, T_{ij} is a turbulent and pressure diffusion term, $P_{ij} = -\overline{u_i u_k}(\partial \overline{U}_j/\partial x_k) - \overline{u_j u_k}(\partial \overline{U}_i/\partial x_k)$ is a production term, $C_{ij} = -2\Omega_m(\epsilon_{mkj}\overline{u_i u_k} + \epsilon_{mki}\overline{u_j u_k})$ is a Coriolis term, Φ_{ij} is a pressure-strain correlation term and ε_{ij} is a dissipation term, respectively.

Introducing the Reynolds stress anisotropy tensor $b_{ij} = \overline{u_i u_j}/2k - \delta_{ij}/3$ and neglecting the diffusive effect, the following relation is derived with Eqs. (9) and (17):

$$\frac{Db_{ij}}{Dt} = \frac{1}{2k}\left(P_{ij} + C_{ij} + \Phi_{ij} - \varepsilon_{ij}\right) - \frac{b_{ij} + \delta_{ij}/3}{k}(P_k - \varepsilon) \tag{18}$$

In the local equilibrium state, since the relation $Db_{ij}/Dt = 0$ holds, Eq. (18) yields the following relation:

$$(P_{ij} + C_{ij} + \Phi_{ij} - \varepsilon_{ij}) = 2\left(b_{ij} + \frac{\delta_{ij}}{3}\right)(P_k - \varepsilon) \tag{19}$$

Using the form $\varepsilon_{ij} = \frac{2}{3}\varepsilon\delta_{ij} +_D \varepsilon_{ij}$ of the dissipation term (Gatski and Speziale, 1993) for Eq. (19), we can obtain

$$\begin{aligned}(P_k - \varepsilon)b_{ij} = &-\frac{2}{3}kS_{ij} - k\left(b_{ik}S_{jk} + b_{jk}S_{ik} - \frac{2}{3}b_{mn}S_{mn}\delta_{ij}\right) \\ &- k[b_{ik}(W_{jk} + 2\epsilon_{mkj}\Omega_m) + b_{jk}(W_{ik} + 2\epsilon_{mki}\Omega_m)] \\ &+ \frac{1}{2}\Pi_{ij}\end{aligned} \tag{20}$$

where $\Pi_{ij} = \Phi_{ij} -_D \varepsilon_{ij}$, and the modeled Π_{ij} is employed as the following general linear model:

$$\begin{aligned}\Pi_{ij} = &-C_1\varepsilon b_{ij} + C_2 kS_{ij} \\ &+ C_3 k\left(b_{ik}S_{jk} + b_{jk}S_{ik} - \frac{2}{3}b_{mn}S_{mn}\delta_{ij}\right) \\ &+ C_4 k(b_{ik}W_{jk} + b_{jk}W_{ik})\end{aligned} \tag{21}$$

where C_1–C_5 are model constants.

Substituting Eq. (21) into (20) and introducing nondimensional quantities, we can obtain the following relation:

$$b^*_{ij} = -S^*_{ij} - \left(b^*_{ik}S^*_{jk} + b^*_{jk}S^*_{ik} - \frac{2}{3}b^*_{k\ell}S^*_{k\ell}\delta_{ij}\right) + b^*_{ik}W^*_{kj} + b^*_{jk}W^*_{ki} \tag{22}$$

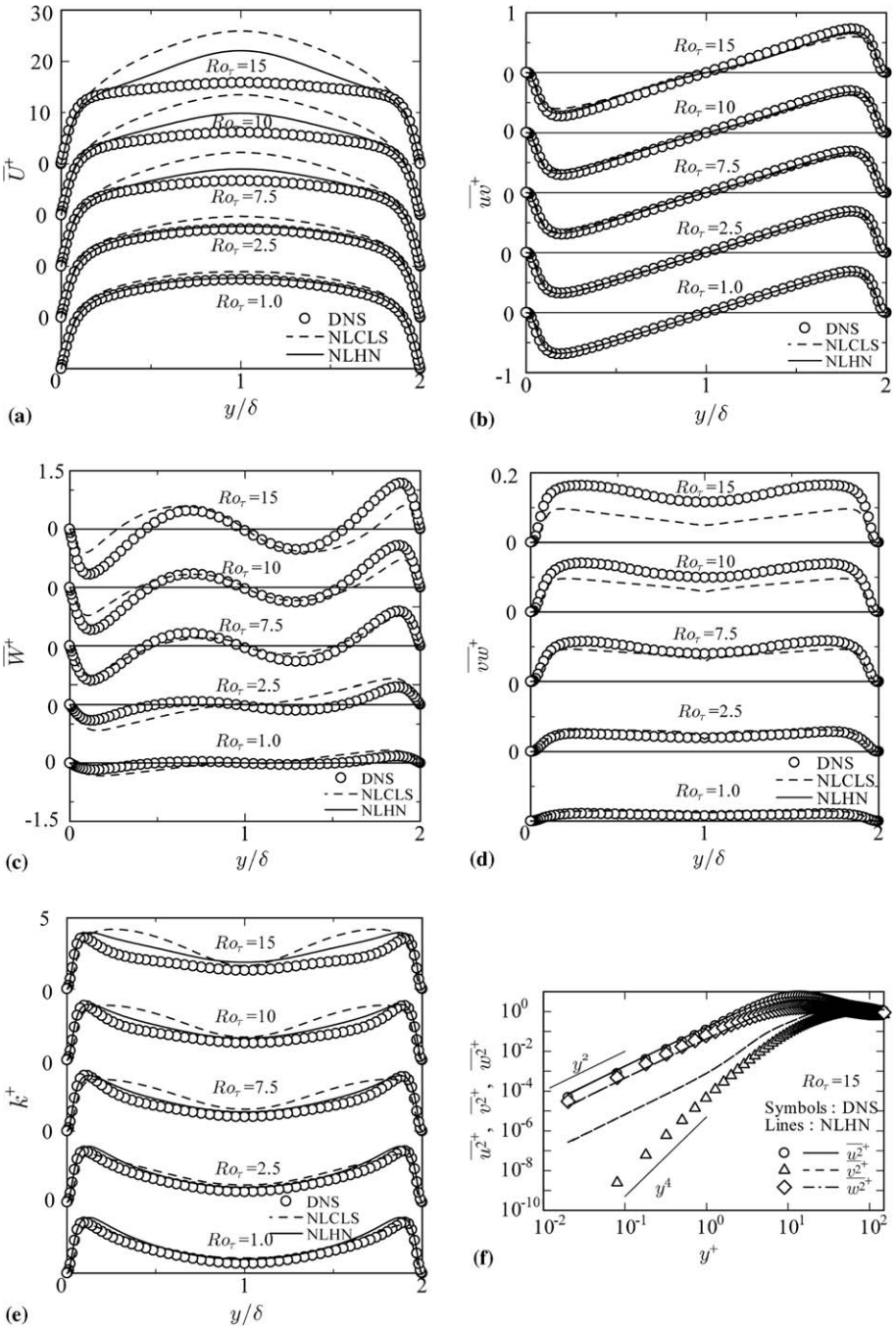

Fig. 4. Evaluations of predicted streamwise rotating flows (Case 1): (a) streamwise mean velocities, (b) Reynolds shear stresses, $\overline{uv}$, (c) spanwise mean velocities, (d) Reynolds shear stresses, $\overline{vw}$, (e) turbulence energy and (f) wall-limiting behaviour of Reynolds stress components.

where

$$\left.\begin{aligned} S^*_{ij} &= \tfrac{1}{2}g\tau(2-C_3)S_{ij}, \quad W^*_{ij} = \tfrac{1}{2}g\tau(2-C_4)\left[\Omega_{ij} + \left(\tfrac{C_4-4}{C_4-2}\right)\epsilon_{mji}\Omega_m\right] \\ b^*_{ij} &= \left(\tfrac{C_3-2}{C_2-\frac{4}{3}}\right)b_{ij}, \quad \tau = \tfrac{k}{\varepsilon}, \quad g = \left(\tfrac{1}{2}C_1 + \tfrac{P_k}{\varepsilon} + \tfrac{G_k}{\varepsilon} - 1\right)^{-1} \end{aligned}\right\} \tag{23}$$

Eq. (23) can be written in the matrix form as

$$\mathbf{b}^* = -\mathbf{S}^* - \left(\mathbf{b}^*\mathbf{S}^* + \mathbf{S}^*\mathbf{b}^* - \frac{2}{3}\{\mathbf{b}^*\mathbf{S}^*\}\mathbf{I}\right) + \mathbf{b}^*\mathbf{W}^* - \mathbf{W}^*\mathbf{b}^* \tag{24}$$

In order to derive an explicit form of $\mathbf{b}^*$ from Eq. (24), the integrity basis, $\mathbf{b}^* = \sum_\lambda Q^{(\lambda)}\mathbf{T}^{(\lambda)}$ first proposed by Pope (1975), is used with the following seven basis tensors:

$$\left.\begin{aligned} \mathbf{T}^{(1)} &= \mathbf{S}^*, & \mathbf{T}^{(6)} &= \mathbf{W}^{*2}\mathbf{S}^* + \mathbf{S}^*\mathbf{W}^{*2} - \tfrac{2}{3}\{\mathbf{S}^*\mathbf{W}^{*2}\}\mathbf{I} \\ \mathbf{T}^{(2)} &= \mathbf{S}^*\mathbf{W}^* - \mathbf{W}^*\mathbf{S}^*, & \mathbf{T}^{(7)} &= \mathbf{W}^*\mathbf{S}^*\mathbf{W}^{*2} - \mathbf{W}^{*2}\mathbf{S}^*\mathbf{W}^* \\ \mathbf{T}^{(3)} &= \mathbf{S}^{*2} - \tfrac{1}{3}\{\mathbf{S}^{*2}\}\mathbf{I}, & \mathbf{T}^{(8)} &= \mathbf{S}^*\mathbf{W}^*\mathbf{S}^{*2} - \mathbf{S}^{*2}\mathbf{W}^*\mathbf{S}^* \\ \mathbf{T}^{(4)} &= \mathbf{W}^{*2} - \tfrac{1}{3}\{\mathbf{W}^{*2}\}\mathbf{I}, & \mathbf{T}^{(9)} &= \mathbf{W}^{*2}\mathbf{S}^{*2} + \mathbf{S}^{*2}\mathbf{W}^{*2} - \tfrac{2}{3}\{\mathbf{S}^{*2}\mathbf{W}^{*2}\}\mathbf{I} \\ \mathbf{T}^{(5)} &= \mathbf{W}^*\mathbf{S}^{*2} - \mathbf{S}^{*2}\mathbf{W}^*, & \mathbf{T}^{(10)} &= \mathbf{W}^*\mathbf{S}^{*2}\mathbf{W}^{*2} - \mathbf{W}^{*2}\mathbf{S}^{*2}\mathbf{W}^* \end{aligned}\right\} \tag{25}$$

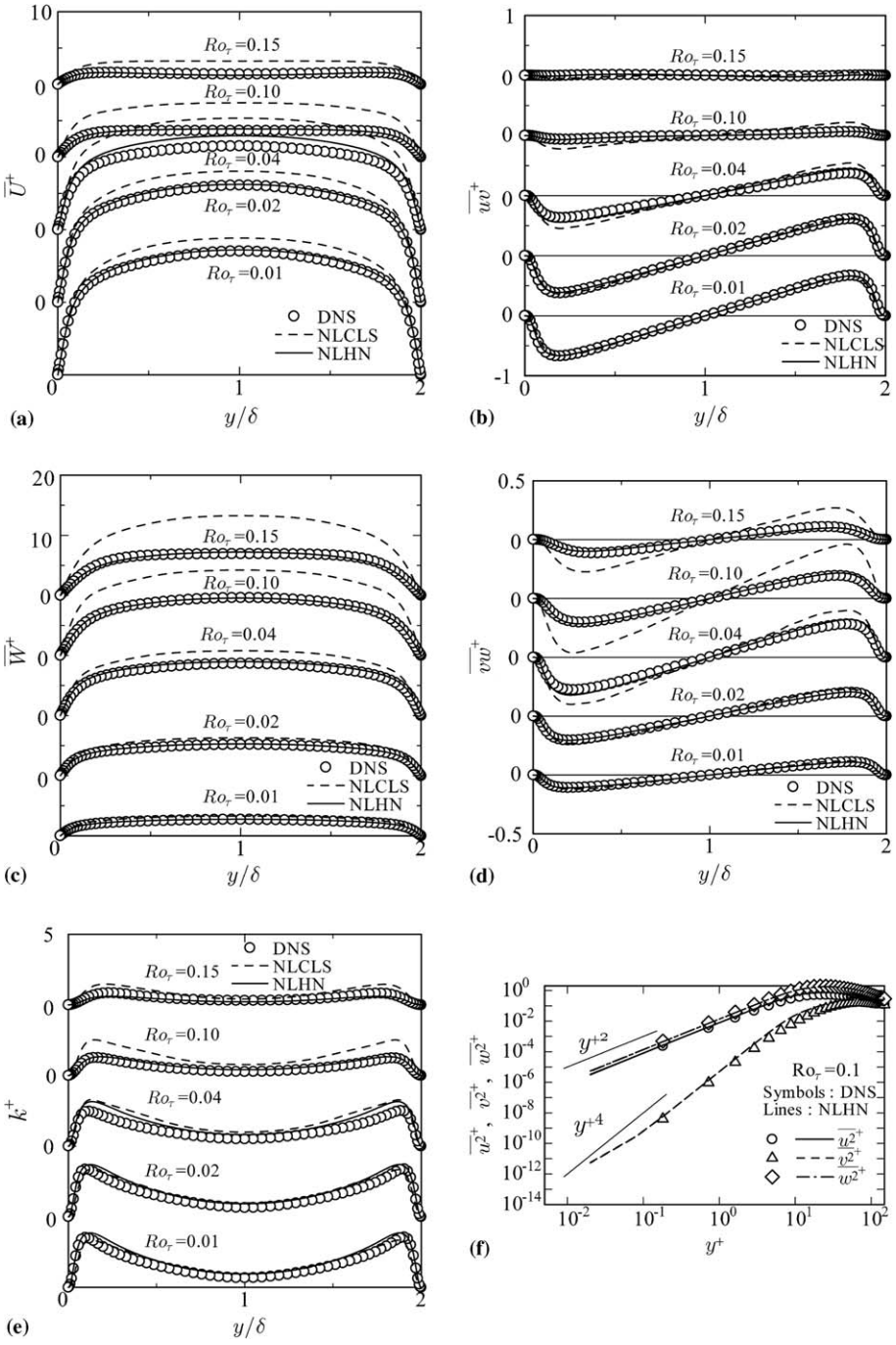

Fig. 5. Evaluations of predicted wall-normal rotating flows (Case 2): (a) streamwise mean velocities, (b) Reynolds shear stresses, $\overline{uv}$, (c) spanwise mean velocities, (d) Reynolds shear stresses, $\overline{vw}$, (e) turbulence energy and (f) wall-limiting behaviour of Reynolds stress components.

Substituting Eq. (25) into $\mathbf{b}^* = \sum_\lambda Q^{(\lambda)}\mathbf{T}^{(\lambda)}$ gives

$$
\begin{aligned}
\mathbf{b}^* &= Q^{(1)}\mathbf{S}^* + Q^{(2)}(\mathbf{S}^*\mathbf{W}^* - \mathbf{W}^*\mathbf{S}^*) \\
&\quad + Q^{(3)}\left(\mathbf{S}^{*2} - \frac{1}{3}\{\mathbf{S}^{*2}\}\mathbf{I}\right) \\
&\quad + Q^{(4)}\left(\mathbf{W}^{*2} - \frac{1}{3}\{\mathbf{W}^{*2}\}\mathbf{I}\right) \\
&\quad + Q^{(5)}\left(\mathbf{W}^*\mathbf{S}^{*2} - \mathbf{S}^{*2}\mathbf{W}^*\right) \\
&\quad + Q^{(6)}\left(\mathbf{W}^{*2}\mathbf{S}^* + \mathbf{S}^*\mathbf{W}^{*2} - \frac{2}{3}\{\mathbf{S}^*\mathbf{W}^{*2}\}\mathbf{I}\right) \\
&\quad + Q^{(7)}(\mathbf{W}^*\mathbf{S}^*\mathbf{W}^{*2} - \mathbf{W}^{*2}\mathbf{S}^*\mathbf{W}^*) \\
&\quad + Q^{(8)}(\mathbf{S}^*\mathbf{W}^*\mathbf{S}^{*2} - \mathbf{S}^{*2}\mathbf{W}^*\mathbf{S}^*) \\
&\quad + Q^{(9)}\left(\mathbf{W}^{*2}\mathbf{S}^{*2} + \mathbf{S}^{*2}\mathbf{W}^{*2} - \frac{2}{3}\{\mathbf{S}^{*2}\mathbf{W}^{*2}\}\mathbf{I}\right) \\
&\quad + Q^{(10)}\left(\mathbf{W}^*\mathbf{S}^{*2}\mathbf{W}^{*2} - \mathbf{W}^{*2}\mathbf{S}^{*2}\mathbf{W}^*\right)
\end{aligned}
\tag{26}
$$

Table 3
Model constants and functions of transport equations for k and ε

$C_{\varepsilon 1}$	$C_{\varepsilon 2}$	$C_{\varepsilon 3}$	$C_{\varepsilon 4}$	$C_{\varepsilon 5}$	C_s	C_ε	C_Ω	$C_{f\Omega}$	f_{t1}	f_{t2}
1.45	1.9	0.02	0.5	0.015	1.4	1.4	−0.045	6.0	$\dfrac{1+9f_w(8)}{[1-f_w(32)]^{1/2}}$	$\dfrac{1+5f_w(8)}{[1-f_w(32)]^{1/2}}$

f_ε	f_Ω	R_Ω
$\left\{1-0.3\exp\left[-\left(\dfrac{R_t}{6.5}\right)^2\right]\right\}[1-f_w^2(3.7)]$	$C_{f\Omega}\exp\left[-\left(\dfrac{R_\Omega}{10}\right)^{0.2}\right]$	$\sqrt{\dfrac{\nu}{\varepsilon}}\sqrt{f_{SW}^{\Omega}}$

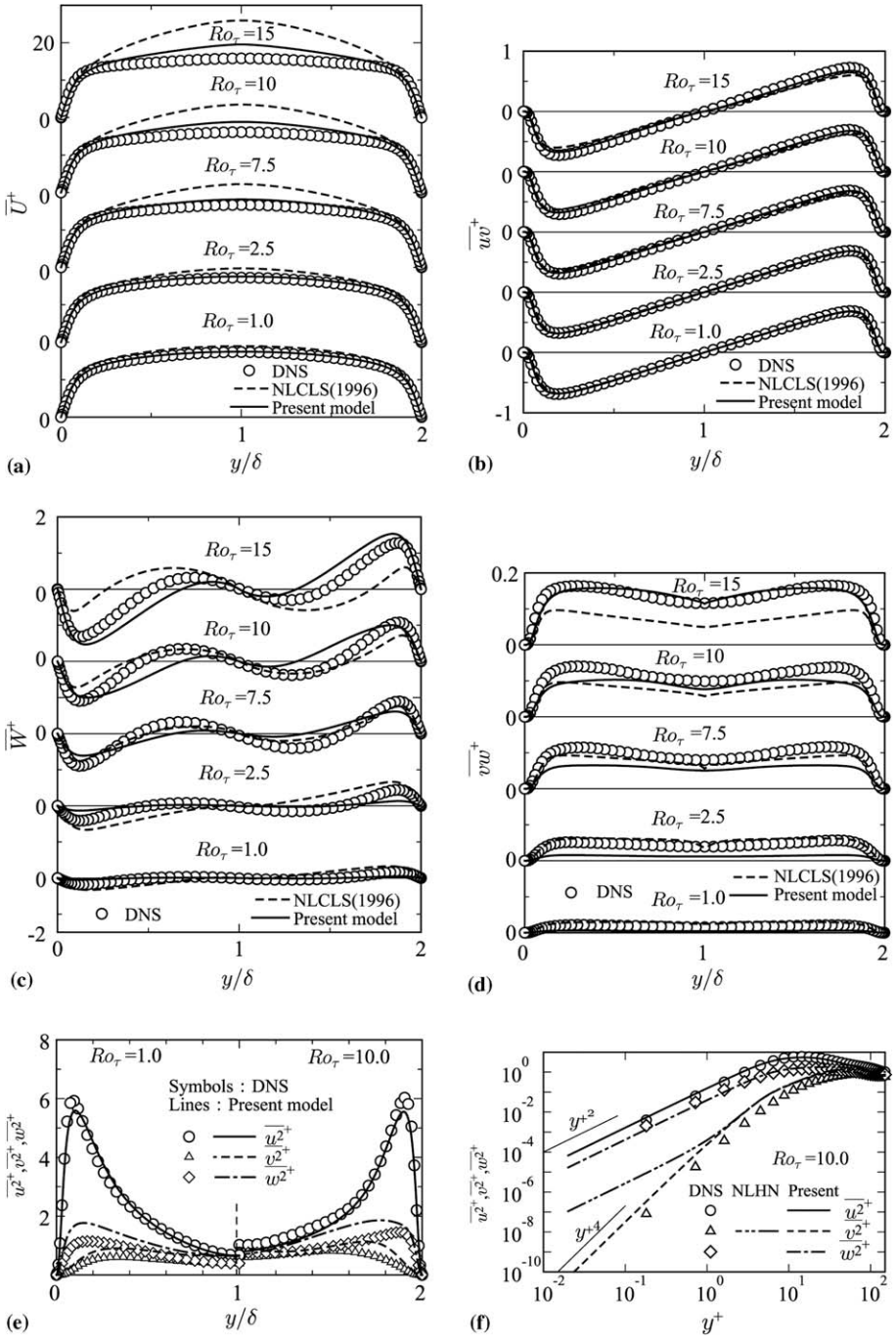

Fig. 6. Distributions of predicted streamwise rotating flows (Case 1): (a) streamwise mean velocities, (b) Reynolds shear stresses, $\overline{uv}$, (c) spanwise mean velocities, (d) Reynolds shear stresses, $\overline{vw}$, (e) turbulent intensities and (f) wall-limiting behaviour of Reynolds stress components.

On the other hand, substituting the integrity basis and the theoretical expressions (Pope, 1975), $\mathbf{T}^{(\lambda)}\mathbf{S}^* + \mathbf{S}^*\mathbf{T}^{(\lambda)} - \frac{2}{3}\{\mathbf{T}^{(\lambda)}\mathbf{S}^*\}\mathbf{I} = \sum_\gamma H_{\lambda\gamma}\mathbf{T}^{(\gamma)}$ and $\mathbf{T}^{(\lambda)}\mathbf{W}^* - \mathbf{W}^*\mathbf{T}^{(\lambda)} = \sum_\gamma J_{\lambda\gamma}\mathbf{T}^{(\gamma)}$ where H and J are the scalar functions, into Eq. (24), gives the following equation for $\mathbf{T}^{(\lambda)}$:

$$\sum_\lambda Q^{(\lambda)}\mathbf{T}^{(\lambda)} = -\sum_\lambda \delta_{1\lambda}\mathbf{T}^{(1)} - \sum_\lambda Q^{(\lambda)}\left[\left(\sum_\lambda H_{\lambda\gamma}\mathbf{T}^{(\lambda)}\right) - \left(\sum_\lambda J_{\lambda\gamma}\mathbf{T}^{(\lambda)}\right)\right] \tag{27}$$

Eq. (27) can be written as $Q^{(\lambda)} = A^{-1}_{\gamma\lambda}B_\lambda$, where $A_{\gamma\lambda} = -\delta_{\lambda\gamma} - H_{\lambda\gamma} + J_{\lambda\gamma}$, and $B_\lambda = \delta_{1\lambda}$. By using Cayley–Hamilton identities, the matrices $H_{\lambda\gamma}$ and $J_{\lambda\gamma}$ can be determined. Thus, we can obtain $Q^{(\lambda)}$ using Mathematica as follows:

$$\left.\begin{aligned} Q^{(1)} &= -\tfrac{1}{2}(6 - 3\eta_1 - 21\eta_2 - 2\eta_3 + 30\eta_4)/D & Q^{(6)} &= -9/D \\ Q^{(2)} &= -(3 + 3\eta_1 - 6\eta_2 + 2\eta_3 + 6\eta_4)/D & Q^{(7)} &= 9/D \\ Q^{(3)} &= (6 - 3\eta_1 - 12\eta_2 - 2\eta_3 - 6\eta_4)/D & Q^{(8)} &= 9/D \\ Q^{(4)} &= -3(3\eta_1 + 2\eta_3 + 6\eta_4)/D & Q^{(9)} &= 18D \\ Q^{(5)} &= -9/D & Q^{(10)} &= 0 \end{aligned}\right\} \tag{28}$$

where

$$D = 3 - \frac{7}{2} + \eta_1^2 - \frac{15}{2}\eta_2 - 8\eta_1\eta_2 + 3\eta_2^2 - \eta_3 + \frac{2}{3}\eta_1\eta_3 - 2\eta_2\eta_3 + 21\eta_4 + 24\eta_5 + 2\eta_1\eta_4 - 6\eta_2\eta_4 \tag{29}$$

with $\eta_1 = \{\mathbf{S}^{*2}\}$, $\eta_2 = \{\mathbf{W}^{*2}\}$, $\eta_3 = \{\mathbf{S}^{*3}\}$, $\eta_4 = \{\mathbf{S}^*\mathbf{W}^{*2}\}$ and $\eta_5 = \{\mathbf{S}^{*2}\mathbf{W}^{*2}\}$.

In order to obtain reasonable forms for $Q^{(1)}$–$Q^{(9)}$, we assume $S_{13} = W_{13} = 0$. Thus, η_3 and η_4 become 0 and $\eta_5 = \frac{1}{2}\eta_1\eta_2$. Therefore, the following reasonable forms for $Q^{(1)}$–$Q^{(6)}$ can be derived:

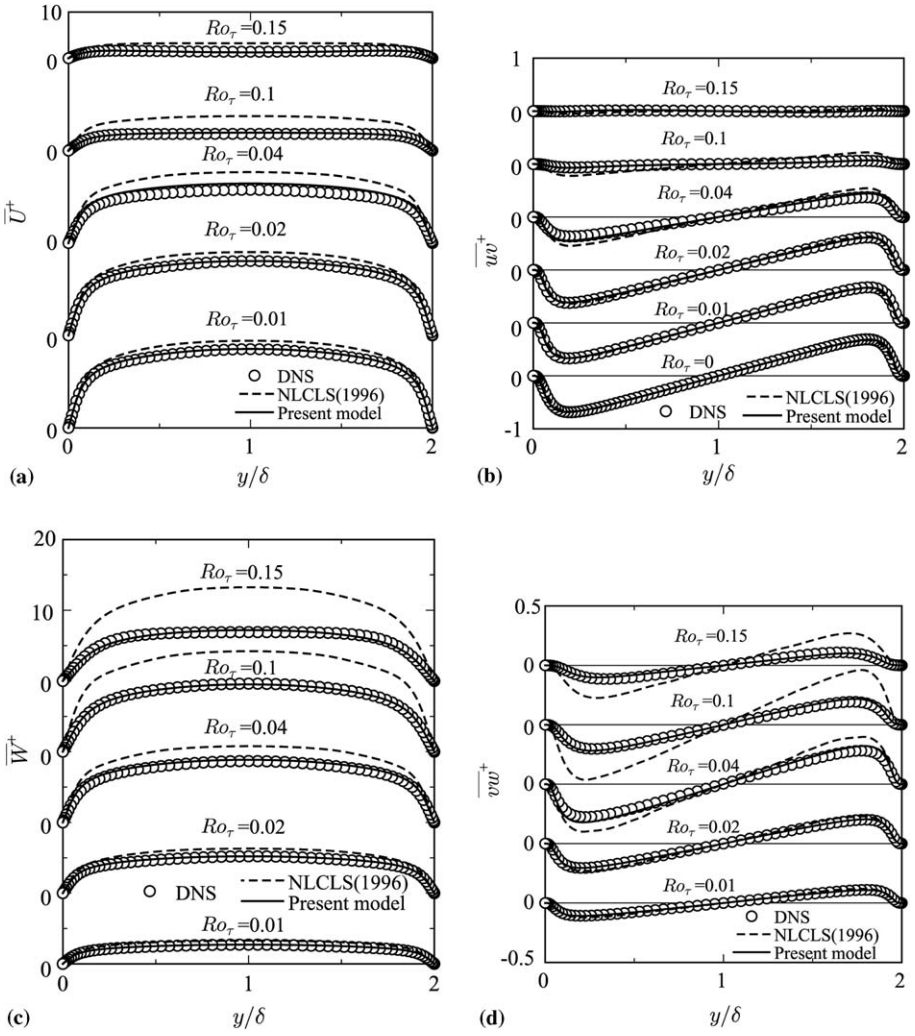

Fig. 7. Distributions of predicted wall-normal rotating flows (Case 2): (a) streamwise mean velocities, (b) Reynolds shear stresses, $\overline{uv}$, (c) spanwise mean velocities and (d) Reynolds shear stresses, $\overline{vw}$.

$$\left.\begin{aligned} Q^{(1)} &= -\tfrac{3}{3-2\eta_1-6\eta_2},\\ Q^{(2)} &= -\tfrac{3}{3-2\eta_1-6\eta_2},\\ Q^{(3)} &= \tfrac{6}{3-2\eta_1-6\eta_2}\\ Q^{(4)} &= \tfrac{-18\eta_1}{(3-2\eta_1-6\eta_2)(2-\eta_1-\eta_2)},\\ Q^{(5)} &= \tfrac{-18}{(3-2\eta_1-6\eta_2)(2-\eta_1-\eta_2)}\\ Q^{(6)} &= \tfrac{-18}{(3-2\eta_1-6\eta_2)(2-\eta_1-\eta_2)} \end{aligned}\right\} \tag{30}$$

Consequently, we can obtain the cubic NLEDM as follows:

$$\begin{aligned} b^*_{ij} = -\frac{3}{3-2\eta^2+6\zeta^2}\Bigg\{ & S^*_{ij} + (S^*_{ik}W^*_{kj} - W^*_{ik}S^*_{kj}) \\ & - 2\left(S^*_{ik}S^*_{kj} - \frac{1}{3}S^*_{mn}S^*_{nm}\delta_{ij}\right) + \frac{6}{2-\eta^2+\zeta^2} \\ & \left[\eta^2\left(W^*_{ik}W^*_{kj} - \frac{1}{3}\delta_{ij}W^*_{mn}W^*_{nm}\right) + (W^*_{ik}S^*_{k\ell}S^*_{\ell j} - S^*_{ik}S^*_{k\ell}W^*_{\ell j})\right. \\ & \left. + \left(W^*_{ik}W^*_{k\ell}S^*_{\ell j} + S^*_{ik}W^*_{k\ell}W^*_{\ell j} - \frac{2}{3}S^*_{\ell m}W^*_{mn}W_{n\ell}\delta_{ij}\right)\right]\Bigg\} \end{aligned} \tag{31}$$

where $\eta = (S^*_{ij}S^*_{ij})^{\frac{1}{2}}$, $\zeta = (W^*_{ij}W^*_{ij})^{\frac{1}{2}}$, and b^*_{ij}, S^*_{ij} and W^*_{ij} are nondimensional quantities, respectively, redefined as follows (Abe et al., 1997):

$$b^*_{ij} = C_D b_{ij}, \quad S^*_{ij} = C_D\tau_{R_o}S_{ij}, \quad W^*_{ij} = 2C_D\tau_{R_o}W_{ij} \tag{32}$$

Since the proposed model in Eq. (31) can be written as the following equation for the Reynolds shear stress, $\overline{vw}$ (or b_{23}), in streamwise rotating flow, in which S_{12} (=S_{21}), W_{12} (=$-W_{21}$), S_{23} (=S_{32}) and W_{23} (=$-W_{32}$) exist, the Reynolds shear stress, $\overline{vw}$, can be reproduced by the present model

$$\begin{aligned} b^*_{23} = \frac{3}{3-2\eta^2+6\zeta^2}\Bigg\{ & S^*_{23} + \frac{6}{2-\eta^2+\zeta^2}[(W^*_{21}S^*_{12}S^*_{23} \\ & - S^*_{21}S^*_{12}W^*_{23}) + (W^*_{21}W^*_{12}S^*_{23} + W^*_{23}W^*_{32}S^*_{23} \\ & + S^*_{21}W^*_{12}W^*_{23} + S^*_{23}W^*_{32}W^*_{23})]\Bigg\} \end{aligned} \tag{33}$$

In Eq. (31), the functions $3/(3-2\eta-2+6\zeta^2)$ and $6/(2-\eta^2+\zeta^2)$ may be taken to be a negative value or 0 with the increase in η. Thus, in order to avoid taking a negative value or 0, we modeled these functions taking into account the rotational effect as follows:

$$\frac{3}{3-2\eta^2+6\zeta^2} \simeq \frac{1}{\left[1+\frac{22}{3}\left(\frac{W^{*2}}{4}\right)+\frac{2}{3}\left(\frac{W^{*2}}{4}-S^{*2}-f^{*2}_\omega\right)f_B+\frac{2}{3}f^{*2}_\omega\right]} \tag{34}$$

$$\frac{6}{2-\eta^2+\zeta^2} \simeq \frac{3}{\left[1+\frac{3}{2}\left(\frac{W^{*2}}{4}\right)+\frac{1}{2}\left(\frac{W^{*2}}{4}-S^{*2}-f^{*2}_\omega\right)f_B+\frac{1}{2}f^{*2}_\omega\right]} \tag{35}$$

where

$$f_B = 1 + C_\eta\left(\frac{W^{*2}}{4} - S^{*2} - f^{*2}_\omega\right) \tag{36}$$

$$f^{*2}_\omega = (C_D\tau_{R_o})^2[\Omega_m(2\epsilon_{mji}W_{ij} - \Omega_m)]^2 \tag{37}$$

The model function, f^{*2}_ω, in Eq. (37) is introduced to avoid an inappropriate value of $(W^{*2}/4 - S^{*2})$ with the increase in a rotational number. Since $f^{*2}_\omega = 0$ is consistently kept in nonrotational flows, inadequate Reynolds stresses predicted by the proposed model are not given in nonrotational flows.

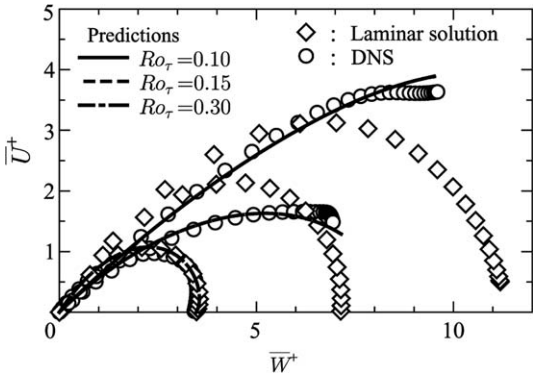

Fig. 8. Relation of between $\overline{U}$ and $\overline{W}$ in wall-normal rotating channel flow.

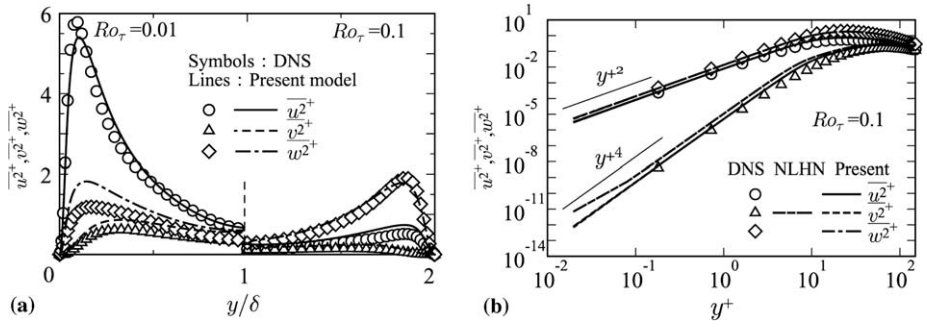

Fig. 9. Distributions of predicted wall-normal rotating flows (Case 2): (a) turbulent intensities and (b) wall-limiting behaviour of Reynolds stress components.

Finally, in order to construct a precise model for rotational flow, a cubic term introduced in an NLCLS model (Craft et al., 1996) is added in the proposed model. Consequently, the final form of the present cubic NLEDM is given as follows:

$$\begin{aligned}\overline{u_iu_j} &= \frac{2}{3}k\delta_{ij} - c_1 v_t S_{ij} + c_2 k(\tau_{R_o}^2 + \tau_{R_w}^2)(S_{ik}W_{kj} - W_{ik}S_{kj}) \\ &+ c_3 k(\tau_{R_o}^2 + \tau_{R_w}^2)\left(S_{ik}S_{kj} - \frac{1}{3}S_{mn}S_{mn}\delta_{ij}\right) \\ &+ c_4 k\tau_{Ro}^2\left(W_{ik}W_{kj} - \frac{1}{3}W_{mn}W_{mn}\delta_{ij}\right) \\ &+ c_5 k\tau_{Ro}^3(W_{ik}S_{k\ell}S_{\ell j} - S_{ik}S_{k\ell}W_{\ell j}) \\ &+ c_6 k\tau_{Ro}^3\left(W_{ik}W_{k\ell}S_{\ell j} + S_{ik}W_{k\ell}W_{\ell j} - \frac{2}{3}S_{\ell m}W_{mn}W_{n\ell}\delta_{ij}\right) \\ &+ c_7 k\tau_{Ro}^3(S_{ij}S_{k\ell}S_{k\ell} - S_{ij}W_{k\ell}W_{k\ell}) \end{aligned} \tag{38}$$

where $v_t = C_\mu f_\mu k^2/\varepsilon$ and $C_\mu = 0.12$, and the model functions and constants are given as follows:

$$\left.\begin{aligned} c_1 &= -2/f_{R1}, \\ c_2 &= -4C_D/f_{R1}, \\ c_3 &= 4C_D/f_{R1}, \\ c_4 &= -8C_D^3 S^2/(f_{R1}f_{R2}) \\ c_5 &= 4C_D^2 f_{R\Omega}/(f_{R1}f_{R2}), \\ c_6 &= 2C_D^2/(f_{R1}f_{R2}), \\ c_7 &= 10C_\mu^2 C_D^2, \quad C_D = 0.8 \\ f_{R1} &= 1 + (C_D\tau_{Ro})^2[(22/3)W^2 \\ &\quad +(2/3)(W^2 - S^2 - f_\omega^2)f_B] \\ f_{R2} &= 1 + (C_D\tau_{Ro})^2[(3/2)W^2 \\ &\quad +(1/2)(W^2 - S^2 - f_\omega^2)f_B] \\ f_{R\Omega} &= 12[1 - \exp(f_{SW}^{3/4}/26)] \\ f_\mu &= [1 - f_w(32)]\{1 + (40/R_t^{3/4}) \\ &\quad \exp[-(R_{tm}/35)^{3/4}]\} \\ f_B &= 1 + C_\eta(C_D\tau_{Ro})^2(W^2 - S^2 - f_\omega^2), \\ f_\omega^2 &= \Omega_m(2\epsilon_{mji}W_{ij} - \Omega_m), \quad C_\eta = 5.0 \end{aligned}\right\} \tag{39}$$

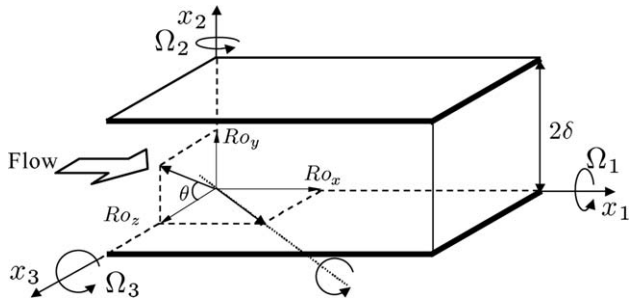

Fig. 10. Coordinate system and arbitrary rotating axis in rotating channel flow.

The characteristic time-scale τ_{R_w} is introduced in an NLHN model (Nagano and Hattori, 2002) for an anisotropy and wall-limiting behaviour of turbulent intensity defined as

$$\tau_{R_w} = \sqrt{\frac{1}{6}\frac{f_{R1}/C_D}{f_{SW}}}\left(1 - \frac{3C_{v1}f_{v2}}{8}\right)f_{v1}^2 \tag{40}$$

$$f_{SW} = \frac{W^2}{2} + \frac{S^2}{3} - f_{SW}^{\Omega} \tag{41}$$

$$f_{SW}^{\Omega} = \left[\left(\sqrt{\frac{S^2}{2}} - \sqrt{\frac{W^2}{2}}\right)f_w(1)\right]^2 \tag{42}$$

where $C_{v1} = 0.4$, $C_{v2} = 2.0\times10^3$, $f_{v1} = \exp[-(R_{tm}/45)^2]$ and $f_{v2} = 1 - \exp\left(-\sqrt{R_t/C_{v2}}\right)$. The wall reflection function is defined by $f_w(\xi) = \exp[-(R_{tm}/\xi)^2]$, and the corrected Reynolds number for the rotating flow is given as $R_{tm} = (C_{tm}n^*R_t^{1/4})/(C_{tm}R_t^{1/4} + n^*)$ with $C_{tm} = 1.3\times10^2$ (Nagano and Hattori, 2002). Moreover, it is found from the evaluation shown in Figs. 4(f) and 5(f) that the wall-limiting behaviour of Reynolds stress component is not satisfied for the tested rotating flows. Thus, the model function in Eq. (42) of characteristic time-scale τ_{R_w} is slightly modified as follows:

$$f_{SW}^{\Omega} = \left|\sqrt{\frac{S^{*2}}{2}} - \sqrt{\frac{W^{*2}}{2}}\right|f_w(1)^2 \tag{43}$$

where $S^* = \epsilon_{\ell mn}S_{mn}\Omega_\ell$, $W^* = \epsilon_{\ell mn}W_{mn}\Omega_\ell$.

For the modeled transport equations of k and ε as indicated in Eqs. (9) and (10), the turbulent diffusion and the pressure diffusion terms are modeled as follows (Nagano and Hattori, 2002):

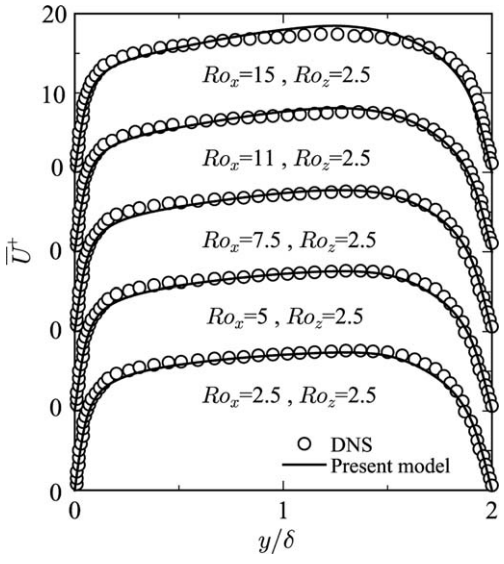

Fig. 11. Distributions of mean velocities in an arbitrary axis rotating channel flow: Case STSP: streamwise mean velocities.

$$T_k = \frac{\partial}{\partial x_j}\left(C_s f_{t1}\frac{v_t}{k}\overline{u_j u_\ell}\frac{\partial k}{\partial x_\ell}\right) \tag{44}$$

$$T_\varepsilon = \frac{\partial}{\partial x_j}\left(C_\varepsilon f_{t2}\frac{v_t}{k}\overline{u_j u_\ell}\frac{\partial \varepsilon}{\partial x_\ell}\right) \tag{45}$$

$$\Pi_k = \max\left\{-0.5\nu\frac{\partial}{\partial x_j}\left[\frac{k}{\varepsilon}\frac{\partial \varepsilon}{\partial x_j}f_w(1)\right], 0\right\} \tag{46}$$

$$\Pi_\varepsilon = C_{\varepsilon 4}\frac{\partial}{\partial x_j}\left\{[1-f_w(5)]\frac{\varepsilon}{k}\frac{\partial \varepsilon}{\partial x_j}f_w(5)\right\} \tag{47}$$

The extra term in the ε-equation is adopted as the identical to the NLHN model (Nagano and Hattori, 2002)

$$E = C_{\varepsilon 3}\nu\frac{k}{\varepsilon}\overline{u_j u_\ell}\frac{\partial^2 \overline{U}_i}{\partial x_\ell \partial x_k}\frac{\partial^2 \overline{U}_i}{\partial x_j \partial x_k} + C_{\varepsilon 5}\nu\frac{k}{\varepsilon}\frac{\partial \overline{u_j u_k}}{\partial x_j}\frac{\partial \overline{U}_i}{\partial x_k}\frac{\partial^2 \overline{U}_i}{\partial x_j \partial x_k} \tag{48}$$

Finally, a rotation-influenced addition term, R, in the ε-equation (10) is generalized as follows:

$$R = C_\Omega f_\Omega k \epsilon_{ij\ell} W_{ij} d_\ell \Omega_\ell \tag{49}$$

where d_ℓ is the unit vector in the spanwise direction. Model constants and functions in the k- and ε-equations are indicated in Table 3.

3.3. Evaluation of proposed model

The evaluations for the newly improved NLEDM are shown in Figs. 6–16. In order to calculate the present model, the numerical technique used is a finite-volume method (Hattori and Nagano, 1995).

First, the predictions of fully-developed streamwise rotating channel flows calculated by the present model are shown in Fig. 6. The results with the NLCLS model (Craft et al., 1996) are also included in the figure for comparison. It can be seen in Figs. 6(a)–(d) that the present model gives accurate predictions of both mean velocities and Reynolds shear stresses in all cases, and the test case of the highest rotational number is adequately reproduced by the present model. Also, the Reynolds normal stresses are indicated in Figs. 6(e) and (f). Now, the present model adequately reproduces redistribution of Reynolds normal stresses, and can predict wall-limiting behaviour exactly. These are because the modified characteristic time-scale τ_{R_w} given as Eq. (40) is introduced in the proposed NLEDM.

Next, cases of wall-normal rotating channel flows are shown in Figs. 7–9. In this case, the streamwise mean velocity decreases with the increasing rotation number due to the exchange momentum between the streamwise and spanwise velocity as indicated in Figs. 7(a) and (c). Thus, the spanwise velocity increases at the lower rotation numbers, but the spanwise velocity reaches maximum value at

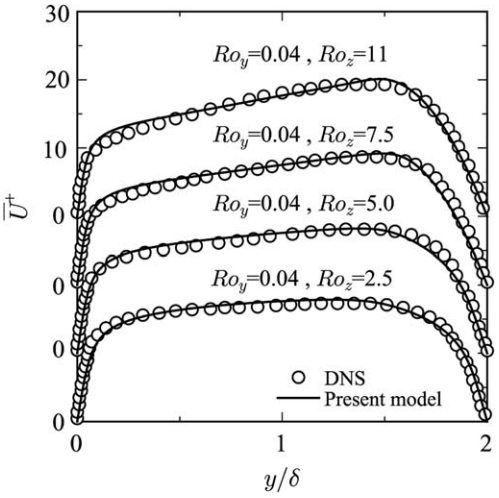

Fig. 13. Distributions of mean velocities in an arbitrary axis rotating channel flow: Case WNSP1: streamwise mean velocities.

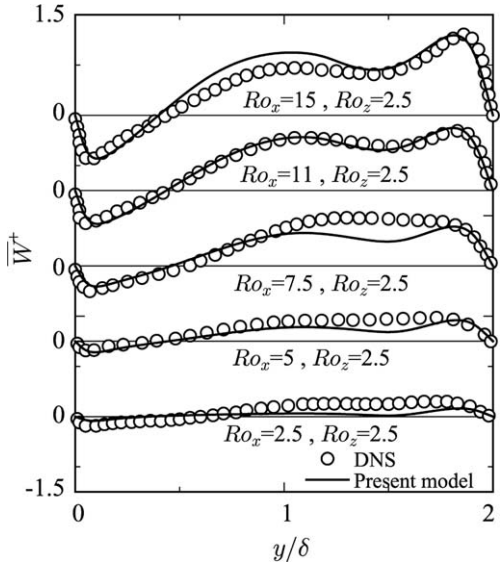

Fig. 12. Distributions of mean velocities in an arbitrary axis rotating channel flow: Case STSP: spanwise mean velocities.

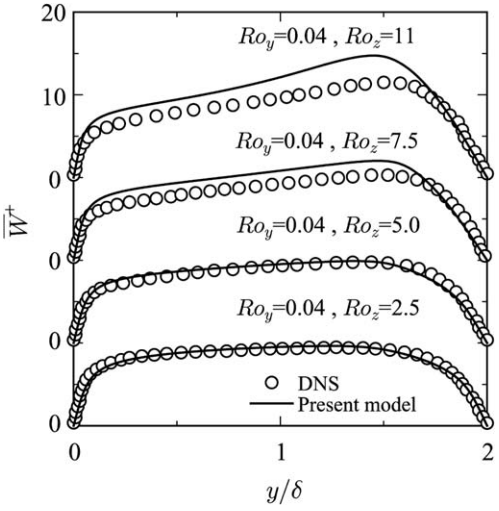

Fig. 14. Distributions of mean velocities in an arbitrary axis rotating channel flow: Case WNSP1: spanwise mean velocities.

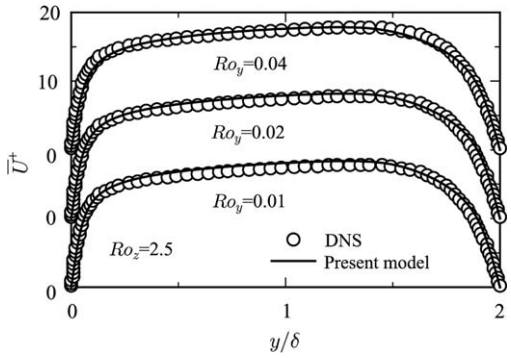

Fig. 15. Distributions of mean velocities in an arbitrary axis rotating channel flow: Case WNSP2: streamwise mean velocities.

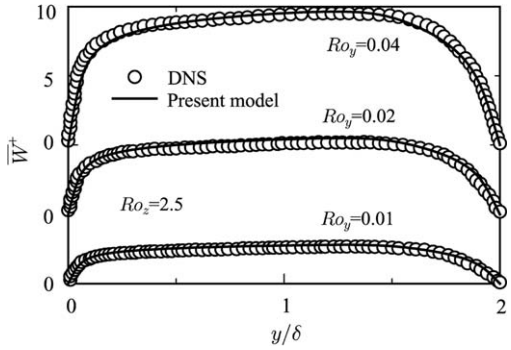

Fig. 16. Distributions of mean velocities in an arbitrary axis rotating channel flow: Case WNSP2: spanwise mean velocities.

a critical rotation number. Then, the spanwise velocity decreases because the streamwise velocity becomes almost zero at higher rotation numbers. In comparison with DNS results, the present model gives better predictions than the predictions of the CLS model. In particular, Reynolds shear stresses, $\overline{vw}$, are predicted very well as shown in Fig. 7(d). Fig. 8 shows relation of between streamwise and spanwise velocities in this case, in which the laminar solutions are included for comparison. Obviously, the flow tends to laminarization with the increasing rotation number, and the present model can predict properly this tendency. Also, the adequate predictions of anisotropy of turbulent intensities are reproduced by the present cubic NLEDM as shown in Fig. 9(a). As the above mentioned, the present model can predict similar to the NLHN model as shown in Fig. 5, but the wall-limiting behaviour is satisfied exactly as indicated in Fig. 9(b). Therefore, it is obvious that the present cubic NLEDM gives higher performance for the predictions of rotating channel flows while maintaining the performance of the basis model, e.g., NLHN model.

Finally, in order to confirm the performance of the present model, cases of rotating channel flow with *combined rotational axes* are calculated as shown in Fig. 10, in which DNS databases of these cases are provided by Wu and Kasagi (2004). The rotation numbers of Case STSP are given as $Ro_{\tau x} = 2.5$–15 and $Ro_{\tau z} = 2.5$, those of Case WNSP1 as $Ro_{\tau y} = 0.04$ and $Ro_{\tau z} = 2.5$–11 and those of Case WNSP2 as $Ro_{\tau y} = 0.01$–0.04 and $Ro_{\tau z} = 2.5$, respectively. The predicted mean velocities are shown in Figs. 11–16 with DNS data (Wu and Kasagi, 2004). It can be seen that the proposed model gives accurate predictions of all cases, since the proper modelling for rotating flows with arbitrary rotating axes is introduced in the present two-equation model with the cubic NLEDM.

4. Conclusions

We have carried out DNSs of various rotation-number channel flows with arbitrary rotating axes in order to obtain fundamental statistics on these flows. It is found from DNS results that cases of streamwise rotating channel flow involve a counter gradient turbulent diffusion regarding spanwise turbulent quantities, so that the linear EDM and the quadratic NLEDM cannot be applied to calculate the case of streamwise rotating channel flow. Using the present DNS data, both the cubic and the quadratic NLEDMs are then evaluated. It is found that the existing models cannot accurately predict turbulent quantities in a streamwise rotating channel flow. Therefore, using the assessment results, we propose a new cubic NLEDM for Reynolds stress modelling in a two-equation turbulence model which can satisfactorily predict rotational channel flows with arbitrary rotating axes. The proposed model can also reproduce anisotropy of turbulent intensity near the wall, and thereby satisfies the wall-limiting behaviour of turbulent quantities in the cases under study.

Acknowledgement

This research was partially supported by a Grant-in-Aid for Scientific Research (S), 17106003, from the Ministry of Education, Culture, Sports, Science and Technology (MEXT), Japan.

References

Abe, K., Kondoh, T., Nagano, Y., 1997. On Reynolds-stress expressions and near-wall scaling parameters for predicting wall and homogeneous turbulent shear flows. Int. J. Heat Fluid Flow 18, 266–282.

Craft, T.J., Launder, B.E., Suga, K., 1996. Development and application of a cubic eddy-viscosity model of turbulence. Int. J. Heat Fluid Flow 17, 108–115.

Gatski, T.B., Speziale, C.G., 1993. On explicit algebraic stress models for complex turbulent flows. J. Fluid Mech. 254, 59–78.

Hattori, H., Nagano, Y., 1995. Calculation of turbulent flows with pressure gradients using a k–ε model. Trans. JSME 59-560B, 1043–11048.

Hattori, H., Nagano, Y., 2004. Non-linear two-equation model taking into account the wall-limiting behavior and redistribution of stress components. Theoret. Comput. Fluid Dyn. 17 (5), 313–330.

Kristoffersen, R., Andersson, H.I., 1993. Direct simulations of low-Reynolds-number turbulent flow in a rotating channel. J. Fluid Mech. 256, 163–195.

Lamballais, E., Lesieur, M., Métais, O., 1996. Effects of spanwise rotation on the vorticity stretching in transitional and turbulent channel flow. Int. J. Heat Fluid Flow 17, 324–332.

Nagano, Y., Hattori, H., 2002. An improved turbulence model for rotating shear flows. J. Turbul. 3 (6), 1–13.

Nagano, Y., Hattori, H., 2003. DNS and modelling of spanwise rotating channel flow with heat transfer. J. Turbul. 4 (10), 1–15.

Oberlack, M., Cabot, W., Rogers, M.M., 1999. Turbulent channel flow with streamwise rotation: Lie group analysis, DNS and modeling. In: Proc. 1st Int. Symp. on Turbulence and Shear Flow Phenomena, pp. 85–90.

Pope, S.B., 1975. A more general effective-viscosity hypothesis. J. Fluid Mech. 72, 331–340.

Wu, H., Kasagi, N., 2004. Effects of arbitrary directional system rotation on turbulent channel flow. Phys. Fluids 16, 979–990.